Modeling the Cannabinoid Receptor: A Three-Dimensional Quantitative Structure-Activity Analysis

BRIAN F. THOMAS, DAVID R. COMPTON, BILLY R. MARTIN, and SIMON F. SEMUS

Department of Pharmacology and Toxicology (B.F.T., D.R.C., B.R.M.) and Division of Biomedical Engineering (S.F.S.), Medical College of Virginia, Virginia Commonwealth University, Richmond, Virginia 23298

Received October 15, 1990; Accepted August 15, 1991

SUMMARY

The structure-activity relationship studies that have been reported for cannabinoids suggest that 1) the conformation of the C-ring at the C9 position, 2) the A-ring phenolic hydroxyl, and 3) the hydrophobic side chain are important determinants for the production of analgesia, as well as other cannabinoid effects. However, either these previous structure-activity studies described for cannabinoid compounds have not been quantitative in nature or the prediction of the activity of known and unknown compounds based on molecular structure has not been tested in a comprehensive manner. In this study we describe a three-dimensional molecular modeling program using comparative molecular field analysis to derive quantitative structure-activity relationships fitting pharmacological potencies and binding affinities of cannabinoids. The analysis has proven to accurately fit the pharmacological activity of cannabinoid analogs, with cross-validated r^2 values of >0.3 and final analysis r^2 values of >0.88. Additionally, this study has further characterized the steric and electrostatic properties that account for the variations in their potency. The results from this study indicate that steric repulsion behind the C-ring is associated with decreased predicted binding affinity and pharmacological potency. On the other hand, the steric bulk of a side chain that is extended up to seven carbons contributes to predictions of increased binding affinity and potency. The electrostatic fields of cannabinoid analogs also contribute to the predicted *in vitro* and *in vivo* potencies. If the biological activities we have investigated are assumed to be the result of interaction with a single binding site, this method indicates the structural and physicochemical properties necessary for binding to the receptor and producing an effect. By defining cannabinoid binding affinity and behavioral activity pharmacophores, this method can be used for designing cannabinoid agonists and it is capable of predicting the activity of unknowns, thereby serving to facilitate rational drug design.

Historically, proposed cellular mechanisms of action for the cannabinoids (e.g., Δ^9-THC) have included nonspecific and specific membrane perturbation (1–3), as well as receptor interaction or modulation (4). The interest in the characterization of a cannabinoid receptor continued despite the slow emergence of supportive data. Cannabinoid binding sites were initially identified in hepatocytes (5) and have been described more recently in the CNS (6, 7). The putative cannabinoid receptor has now been cloned and the cDNA shown to express functional binding sites in N18TG-2 and NG108-15 cell lines (8). Despite this recent acceleration of research findings regarding the receptor-mediated mechanism of action of cannabinoids, there is relatively little direct knowledge regarding the structure of this putative receptor in the CNS. The purification and characterization of cannabinoid binding sites in the CNS, as well as the identification of endogenous ligands, are, therefore, areas of current investigation. Because the receptor substance has not

been purified and analyzed for its three-dimensional structure and shape, there is little direct knowledge as to the nature of the ligand-receptor interaction. In such a case, it is only possible to derive a model of the receptor (based on the comparison of structural features of known active and inactive molecules) that provides a consistent explanation of the observed data and, ideally, one that should predict the potency of compounds yet to be synthesized.

It has been established that there are strict structural requirements for cannabinoid behavioral effects (9, 10). Speculation regarding the portions of Δ^9-THC that are involved in receptor recognition and activation usually implicates the C9 position, the phenolic group at C1, and the side chain at C3 (11–13). These structural requirements may be used as molecular features that can be compared in structurally diverse compounds. Once orientation and alignment rules have been defined as a basis for the comparison of noncongeneric molecules, it should be possible to associate the locality of molecular fragments with changes in biological potency. New statistical techniques that are capable of handling large numbers of variables and a limited

---

ABBREVIATIONS: THC, tetrahydrocannabinol; CNS, central nervous system; QSAR, quantitative structure-activity relationship; CoMFA, comparative molecular field analysis; PLS, partial least-squares analysis; log $P_{o/w}$, logarithm of the n-octanol/water partition coefficient.

set of observations have stimulated the development of novel approaches in the determination of QSARs. One such approach is CoMFA, which samples the steric and electrostatic fields surrounding a set of ligands by interaction with a charged probe atom (14).

CoMFA relies on the observation that the interaction between molecule and receptor leading to an observed biological response is usually noncovalent in nature and that a variety of the molecular properties can be accounted for by the use of molecular mechanics force fields. Such force fields treat noncovalent interactions only in terms of their steric and electrostatic interactions, and it is that limitation that is placed upon the molecular field analysis. Thus, the comparison of the steric and electrostatic fields surrounding a series of molecules, together with data analysis by PLS and cross-validation methodologies, maximizes the likelihood that the results will have predictive value (15).

Of primary importance in a comparative molecular field analysis is the definition of a set of alignment rules for the series of compounds under investigation. The postulation of such a set of rules is left to the chemical intuition of the investigator. Molecules are then modeled and aligned to satisfy the defined rules. A grid, or cage, is then calculated as a box of points in the theoretical receptor space surrounding the aligned molecules, and the steric and electrostatic fields are calculated that each molecule would exert upon a probe atom placed at each grid point. After data analysis by PLS, with cross-validation, the alignment of the most poorly predicted compounds may be adjusted slightly and the analysis repeated, until a mutual alignment is found that produces a three-dimensional QSAR possessing the highest correlation between predicted and actual activity (16). The QSAR coefficients are displayed as contour plots around the aligned molecules, enabling the visualization of those regions where changes in the steric and electrostatic fields have the greatest influence on the predicted biological potency. The analysis may then be used for the prediction of the properties of modeled compounds that have not yet been synthesized. The synthesis and biological evaluation of compounds predicted to be pharmacologically active can then be used to assess and refine the model. Therefore, the predictive power of CoMFA analyses can assess how robust the QSAR model is and may also be useful in suggesting potential alignments when the unknown molecule is not easily fit to the template molecule.

The development of CoMFA allows a novel approach to be used for developing pharmacophores and QSAR equations. Other techniques, such as the active analog approach, allow for the prediction of the biologically active conformation of analogs based upon prior determination of the pharmacophore. This method uses the searching of conformational space of the most rigid analogs and application of distance constraints from that determination to searches of more flexible molecules. The active analog approach can be additionally used in essential volume mapping, whereby the cumulative volumes of active analogs are subtracted from those of the inactive analogs, to give the receptor's "essential volume." This method of analysis typically produces either an "active" or "inactive" prediction, whereas CoMFA allows more quantitative predictions of unknowns. The active analog approach has been used in defining alignment rules for subsequent use in CoMFA (17). However, this technique for conformational determination is not applicable to this study of the cannabinoids, which contain structures that are predominantly rigid or are characterized by relatively little rotational freedom around relevant bonds.

In the present work, a three-dimensional structure-activity analysis of the relationship between the physicochemical properties of 33 cannabinoid compounds and their potencies in four behavioral assays and their IC_{50} values in an *in vitro* binding assay is described. The octanol/water partition coefficients of each compound (as $\log P_{o/w}$ values) were included in the QSAR, due to the large amount of literature suggesting that both nonspecific and specific membrane perturbation occurs with cannabinoids (1–3, 18–20). Although lipophilicity is not directly related to cannabinoid potency (21), the $\log P_{o/w}$ values were included to assess whether lipophilicity contributes to cannabinoid potency when steric and electrostatic factors were also considered. The QSAR table was, therefore, comprised of 33 rows for the cannabinoid analogs and seven columns containing the CoMFA data, the $\log P_{o/w}$ values, the IC_{50} values in a competitive binding assay with [^{3}H]CP-55,940, and the ED_{50} values for producing changes in locomotor activity, rectal temperature, antinociception, and ring-immobility. The models developed by this analysis yielded high correlation coefficients for predicting the potency of each compound in pharmacological and binding affinity assays of cannabinoids. The results of this analysis show that the molecular properties of cannabinoid compounds can be evaluated by molecular mechanics force fields to elucidate three-dimensional QSAR. Assuming that all pharmacological responses are produced from cannabinoid interaction with the same binding sites in a single binding conformation or orientation, the results of this analysis may be interpreted with respect to the geometric and electrostatic properties of the receptor (22).
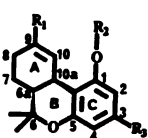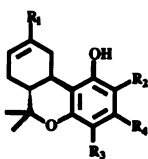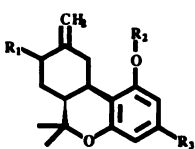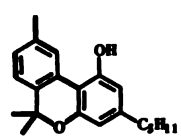
Methods
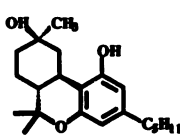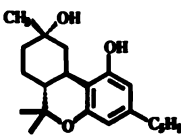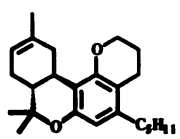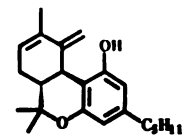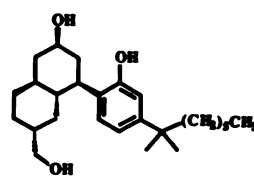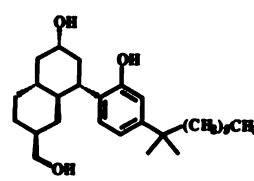
Molecular models and energy minimization. The structures of cannabinoid analogs that were incorporated into the analysis (Table 1) were modeled using the SYBYL 5.4 molecular modeling package (Tripos Associates, Inc., St. Louis, MO). The initial structures were generated using CONCORD, which produced three-dimensional structures directly from a SMILES input (Simplified Molecular Input Line Entry System). Atomic charges were calculated for all molecules (Gasteiger-Hückel method), and structure energies were minimized using the Tripos force field. The minimization process modified the geometry of the molecule until the energy difference between successive iterations was <0.005 kcal/mol. CONCORD generates only a single conformer, without complete conformational sampling with respect to energy. Therefore, in those molecules where several areas of conformational space could be occupied, searches were performed in 1° increments around relevant rotatable bonds, in order to determine the global minimum energy conformation. The final structures of all molecules were energy minimized again after conformational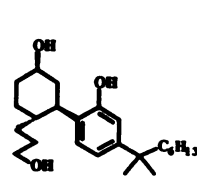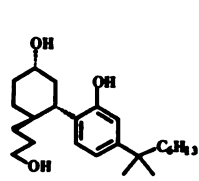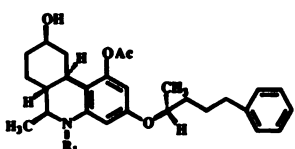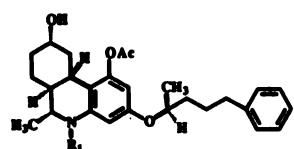 searching until the energy difference between successive iterations was <0.005 kcal/mol. Because one assumption that must be made for any molecule present in a QSAR analysis is that of metabolic stability, the four nantradol compounds (levo-, dextro-, *N*-methyl-levo-, and *N*-methyl-dextro-nantradol) were modeled as the desacetylated active metabolites.

Alignment and measurement of molecular fields. Because all compounds in this analysis possessed an aromatic ring and an aliphatic side chain, the compounds were aligned so as to superimpose these groups. The side chains of the compounds were then rotated so that they were superimposed with the side chain of Δ^9-THC. In the case of CP-55,940, the *n*-propyl alcohol group was aligned with respect to its restricted analog CP-55,243. The alignment of the aromatic rings and side chains served to position the compounds in similar orientations in space, so that a lattice could be placed around the compounds with a 2-Å spacing between sampling points. This grid, large enough to encom-

TABLE 1

Structure and lipophilicty (log $P_{o/w}$) of cannabinoid analogs

The structures of the natural and synthetic cannabinoid analogs that were incorporated into the QSAR analysis are shown, with the numbering system for Δ⁹-THC and ring systems designated where appropriate.

| | | | Δ⁸-THC analogs | | Δ⁹⁻¹¹-THC analogs | |
| | | | | | | |

Compound	Δ	R_1	R_2	R_3	R_4	$P_{o/w}$
Δ⁹-THC	9	CH_3	H	$(CH_2)_4CH_3$		6.98[a]
Δ⁹-THC-methyl ether	9	CH_3	CH_3	$(CH_2)_4CH_3$		7.75[b]
11-OH-Δ⁹-THC-DMH[c]	9	CH_2OH	H	$CH(CH_3)_2C_6H_{13}$		7.83[a]
11-Oxo-Δ⁹-THC-DMH	9	COH	H	$CH(CH_3)_2C_6H_{13}$		8.03[a]
9-COOH-Δ⁹-THC-DMH	9	COOH	H	$CH(CH_3)_2C_6H_{13}$		7.37[b]
Δ⁸-THC	8	CH_3	H	H	$(CH_2)_4CH_3$	7.41[a]
Δ⁸-THC-DMH	8	CH_3	H	H	$CH(CH_3)_2C_6H_{13}$	9.97[a]
(−)-11-OH-Δ⁸-THC-DMH	8	CH_2OH	H	H	$CH(CH_3)_2C_6H_{13}$	7.44[a]
(+)-11-OH-Δ⁸-THC-DMH	8	CH_2OH	H	H	$CH(CH_3)_2C_6H_{13}$	7.44[a]
9-COOH-Δ⁸-THC	8	COOH	H	H	$(CH_2)_4CH_3$	5.51[b]
5′-Bromo-Δ⁸-THC	8	CH_3	H	H	$(CH_2)_4CH_2Br$	7.03[b]
5′-Iodo-Δ⁸-THC	8	CH_3	H	H	$(CH_2)_4CH_2I$	7.42[b]
5′-Trifluoro-Δ⁸-THC	8	CH_3	H	H	$(CH_2)_4CF_3$	6.59[b]
2-Nitro-Δ⁸-THC	8	CH_3	NO_2	H	$(CH_2)_4CH_3$	7.34[b]
4-Nitro-Δ⁸-THC	8	CH_3	H	NO_2	$(CH_2)_4CH_3$	7.34[b]
2,4-Dinitro-Δ⁸-THC	8	CH_3	NO_2	NO_2	$(CH_2)_4CH_3$	7.15[b]
11-Fluoro-Δ⁸-THC	8	CH_2F	H	H	$(CH_2)_4CH_3$	6.45[b]
2-Iodo-Δ⁸-THC	8	CH_3	H	H	$(CH_2)_4CH_3$	8.30[b]
8-β-OH-Δ⁹⁻¹¹-THC	9–11	OH	H	$(CH_2)_4CH_3$		5.09[a]
Δ⁹⁻¹¹-THC	9–11	H	H	$(CH_2)_4CH_3$		7.18[b]

Cannabinol
log $P_{o/w}$ = 7.39[b]

9-β-OH-HHC[d]
log $P_{o/w}$ = 5.64[b]

9-α-OH-HHC
log $P_{o/w}$ = 5.64[b]

O,2-Proprano-Δ⁸-THC
log $P_{o/w}$ = 8.30[b]

10-Methylene-Δ⁸-THC
log $P_{o/w}$ = 7.33[b]

CP-55,244
log $P_{o/w}$ = 6.13[b]

CP-55,243
log $P_{o/w}$ = 6.13[b]

CP-55,940
log $P_{o/w}$ = 6.07[b]

CP-56,667
log $P_{o/w}$ = 6.07[b]

| | Levonantradol analogs | | Dextronantradol analogs | |
Compound		R_1		log $P_{o/w}$
Levonantradol		H		5.07[b]
N-Methyl-levonantradol		CH_3		5.70[b]
Dextronantradol		H		5.07[b]
N-Methyl-dextronantradol		CH_3		5.70[b]

[a] Values determined by high pressure liquid chromatography.
[b] Values calculated using CLOGP-3 (see Methods).
[c] DMH, 1,1-dimethylheptyl.
[d] HHC, hexahydrocannabinol.

pass all of the compounds in the series, served to position a probe atom (sp^3 carbon with a +1 charge) around the molecules at all lattice intersection points so that the steric (van der Waals) and electrostatic (coulombic) interactions between the molecule and the probe atom could be quantified. Wherever the probe atom encountered a steric repulsion of >30 kcal/mol (e.g., inside the molecules' volume), the steric interaction is set to that value as a cutoff. The resulting steric and electrostatic forces exerted by each molecule on the probe atom were then incorporated into the QSAR analysis.

QSAR parameters. The potency of each compound was input into the QSAR table as the logarithm of the ED_{50} (μmol/kg). Compounds that were not active in a behavioral assay at the doses tested were given the ED_{50} value corresponding to the highest dose tested. The pharmacological potencies of these analogs have been previously reported (23, 24) or have been submitted for publication.[1] The binding affinities as determined in a competitive binding assay using [^{3}H]CP-55,940 (data to be published elsewhere) were input as log IC_{50} values (nM) with a cutoff value of 10 μM.[1] The log $P_{o/w}$ of each analog was either determined experimentally by reverse phase high pressure liquid chromatography (21) or calculated based on molecular structure using CLOGP-3 (MedChem Software 3.54; Daylight Chemical Information Systems, Inc., Claremont, CA). The QSAR table was, therefore, composed of 33 rows representing the cannabinoid analogs and seven columns containing the CoMFA data, the log $P_{o/w}$ values, the IC_{50} values, and the ED_{50} values for producing changes in locomotor activity, rectal temperature, antinociception, and ring-immobility. It is important to note that the CoMFA column actually contains many columns representing the steric and electrostatic field exerted by the compounds at each lattice point.

QSAR analysis. The initial analysis of the QSAR table was performed using a cross-validated PLS analysis to determine the optimal number of components in the model and also the robustness of the model (i.e., the degree to which the predictive power of the model is influenced by the presence of one or a small number of compounds being present in the development of the model). Because of the unusually proportioned table containing many more columns than rows, PLS with cross-validation was required in order to minimize the possibility that erroneous correlations were reported. The number of components in the equation was increased as long as the resulting cross-validated r^2 increased, with a maximum number of components in the equation explaining activity set at five. Increasing the number of components results in an increasingly complex model for explaining the potency of the compounds and also lowers its robustness. The number of cross-validation groups was chosen that specified that a training set that contained approximately 80% of the compounds would be randomly selected from the QSAR table. This table was then used to derive an equation predicting the activity of the compounds in this training set. The pharmacological potencies of the compounds that had been omitted from the training set were then predicted and compared with their observed potencies. This process was repeated until each compound had been incorporated into the cross-validation subtable and its potency predicted by the model obtained based on the training set. The sum of squared differences between predicted and actual potencies was compared with the standard deviation of the actual potencies, to obtain a cross-validated r^2. Once the optimal number of components had been determined through the cross-validation process, the analysis was repeated, setting the number of components to the optimal value and the number of cross-validation groups to zero. Thus, by setting the number of components to the optimum, and specifying no cross-validation, a final analysis was performed where the model derived was based upon all the compounds in the QSAR table.

Comparison of fields. The important steric and electrostatic features of the QSAR determined through the CoMFA analysis were graphically depicted by plotting the product of the coefficients and the standard deviation of the CoMFA column data. These contour plots

enable the electrostatic and steric properties associated with changes in the pharmacological potency to be visualized three-dimensionally. The plots were generated so that contours that are green indicate areas where steric bulk of cannabinoid analogs is strongly associated with increased potency and contours that are blue are areas that are also associated with increased potency, but to a lesser degree than those in green. In contrast, red contours indicate areas where steric forces are highly correlated with decreased pharmacological potency. Yellow contours are also associated with decreased potency but weighted less than contours in red. The contour plots of the electrostatic forces associated with changes in potency were generated so that positive charge should be moved closer to areas contoured in green and blue and farther from regions of red and yellow (assuming that a larger value of the target property is desired). The steric and electrostatic contour plots (indicating structure-activity relationships) were determined for the potency in each pharmacological assay and for binding affinity, to allow comparison among pharmacophores.

Predictions. The ability of the model to predict the potency of compounds not included in the training set was tested using cannabinoid-induced behavioral activities as the target properties. Compounds were modeled, energy minimized, and aligned to Δ^9-THC as previously described. The compounds that were predicted are shown in Fig. 7. Both 11-Br-Δ^8-THC and CP-58,437-1 were modeled as their desacetylated metabolites. The logarithm of the predicted potency was plotted against the actual potency (μmol/kg) (actual potency unknown until after the predictions had been made) and analyzed using least squares linear regression. An additional prediction was made on a compound that has yet to be synthesized.

Results

Molecular models and energy minimization. The molecular models of four of the cannabinoid analogs and their superposition are shown in Fig. 1. In the case of the prototype compound, Δ^9-THC (Fig. 1A), a conformational search of the side chain indicated four minimum energy conformations, and the side chain was thus arbitrarily oriented in one of these four minimum energy conformations. This user-defined orientation was necessary because analogs that restrict the rotation of the side chain that were modeled in this study have not been tested in the four behavioral assays in mice. The rotation of the ring systems of CP-55,243 (Fig. 1B) revealed two energy minima, separated by relatively large rotational energy barriers (data not shown). Because the rotational energies for the AC and ACD ring structures of these compounds were similar, the bicyclic compound CP-55,940 (Fig. 1C) was oriented to overlap with CP-55,243 and the stereoisomers CP-56,667 (Fig. 1D) and CP-55,240, generated by inverting the chiral carbons. The alignment of these four compounds is shown in Fig. 2.

QSAR analysis. The cross-validation analysis of the relationship between the cannabinoids' molecular fields and their behavioral activity determined that the optimal number of components in the equation predicting potency was five and yielded cross-validated r^2 values of 0.65, 0.50, 0.60, and 0.62 for the locomotor activity, tail-flick, rectal temperature, and ring-immobility assays, respectively. The cross-validated r^2 obtained for the binding affinities of 25 of the cannabinoid analogs was the lowest value, 0.31, obtained with an equation with four components. The cross-validated r^2 is defined as:

$$r^2 = (\text{standard deviation} - \text{press})/\text{standard deviation}$$

where the standard deviation is the sum of the squared deviations of each biological potency value from their mean, and press is the sum, over all compounds, of the squared differences between the actual and predicted biological potency values. The
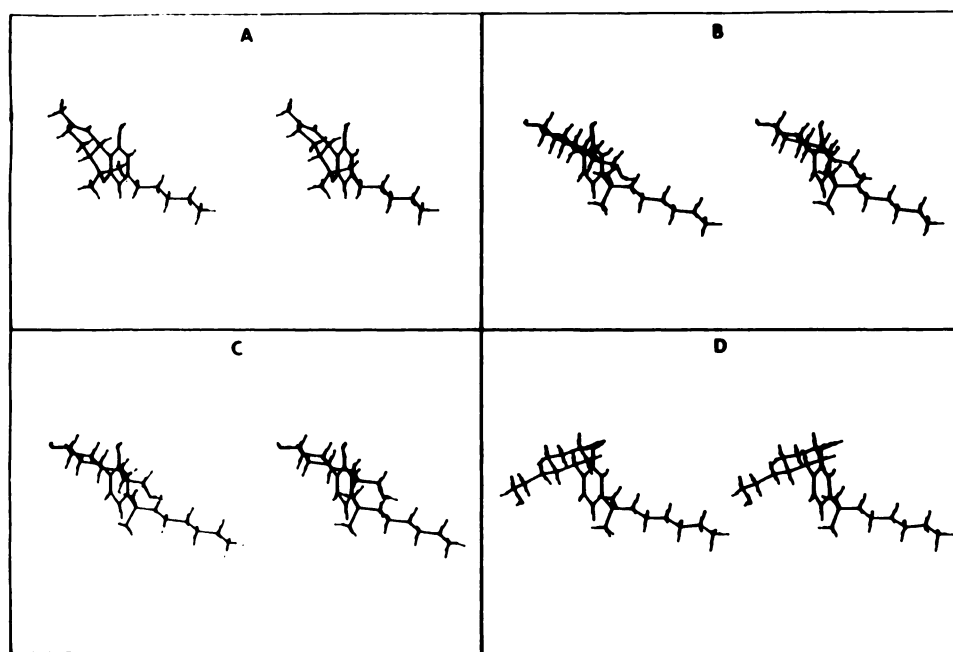
Fig. 1. Stereoviews of the energy-minimized structures of Δ^9-THC (A), CP-55,244 [(−)-ACD] (B), CP-55,940 [(−)-AC] (C), and CP-56,667 [(+)-AC] (D).

final analysis (based on all cannabinoids present in the QSAR table) with behavioral activities as the dependent variables, and given the optimal number of five components, increased the r^2 values to 0.91, 0.88, 0.90, and 0.91 (correlation coefficients of 0.95, 0.93, 0.95, and 0.96) for cannabinoid-induced changes in spontaneous activity, tail-flick, rectal temperature, and ring-immobility, respectively, as shown in Fig. 3. The final analysis with binding affinities as the dependent variable and a four-component model resulted in a correlation coefficient of 0.96 (data not shown).

Comparison of fields. Contour plots of the product of the field coefficients multiplied by the CoMFA columns' standard deviation, plotted in three-dimensional space around the aligned molecules, enable the visualization of regions where changes in the steric properties of analogs (Fig. 4) are correlated with experimentally determined differences in biological potency (hypothermia). Δ^9-THC is shown inside the contour plot to aid in visualization of the results. The steric plot shows areas where decreases in potency are associated with the presence of steric bulk (contoured in red) behind the plane of the aromatic ring at the C11 position of Δ^9-THC and in front of the plane of the aromatic ring at the *gem*-dimethyl groups. These areas correspond to the volume occupied by the inactive isomers of the AC and ACD analogs, the inactive nantradol isomers, and other cannabinoid compounds present in the table. Other small areas contoured in red are present at the phenolic hydroxyl and above the C11 position of Δ^9-THC, coinciding with the volume occupied by the methyl ether derivative of Δ^9-THC and the carboxylic acid groups of Δ^9- and Δ^8-THC analogs, respectively. The areas contoured in red are surrounded by contours in yellow, indicating the relative importance of these areas for predicting decreased potency. Areas that are contoured only in yellow are seen below the C4 position and behind the plane of the aromatic ring at the C2′ position (coinciding with areas occupied by the nitro group of both the 2,4-dinitro and the 4-nitro analogs of Δ^8-THC and the side chain methyl group of both dextronantradol and *N*-methyldextronantradol, respectively). Areas that are contoured in green (where increases in the steric field of cannabinoid molecules are associated with increased potency) are seen at the end of the side chain (C5′).

This area coincides with molecules that have additional atoms attached to the C5′ position of Δ^9-THC, such as the dimethyl-heptyl side chain-containing analogs. These areas are surrounded by contours in blue, indicating that this is an important area contributing to the model's predictive power. There are also blue contours at the C11 position of Δ^9-THC, indicating that compounds with methyl or hydroxyl groups attached to C9 are predicted to be more potent in producing hypothermia than carboxylic acids (which extend beyond these blue contours into the area contoured in yellow and red).

In the electrostatic plot, potency changes are indicated in a similar fashion as those discussed for the steric plots. The contour plot of the electrostatic field (Fig. 5) indicates where electrostatic fields were determined by the QSAR analysis to affect cannabinoid potency in the hypothermia assay. This map is characterized by blue contours at the location corresponding to the oxygen in the pyran ring system, behind the plane of the aromatic ring at the C11 position, and in front of the plane of the aromatic ring at the C11 position of Δ^9-THC. A green region is also seen within a blue contour at the C11 position. A large volume contoured in red is found between these areas, located directly above the C11 position. These areas indicate the importance of the position of substituents at areas coinciding with the C11 position of Δ^9-THC in predicting the potency of cannabinoid analogs. The green and blue contours behind the C11 position correspond to C11-hydroxylated analogs, whereas the blue contour in front of the C11 position corresponds to the hydroxyl groups in CP-55,940 and CP-55,244. The red and yellow contours correspond to the hydroxyl groups of the carboxylic acid analogs of Δ^8- and Δ^9-THC analogs. Thus, the green and blue contours indicate that, in order to increase the predicted potency of analogs, functional groups containing protons (i.e., OH, NH, etc.) should be positioned so as to extend into these areas and not into the area directly above the C11 position.

Predictions. The results of the predictions indicate that the models derived for behavioral potency can accommodate such structurally diverse compounds as the (+)-isomer of 11-OH-Δ^9-THC-DMH, as well as the aminoalkylindoles WIN-55212-2 [(+)-isomer] and WIN-55212-3 [(−)-isomer] (Fig. 7), as evi-
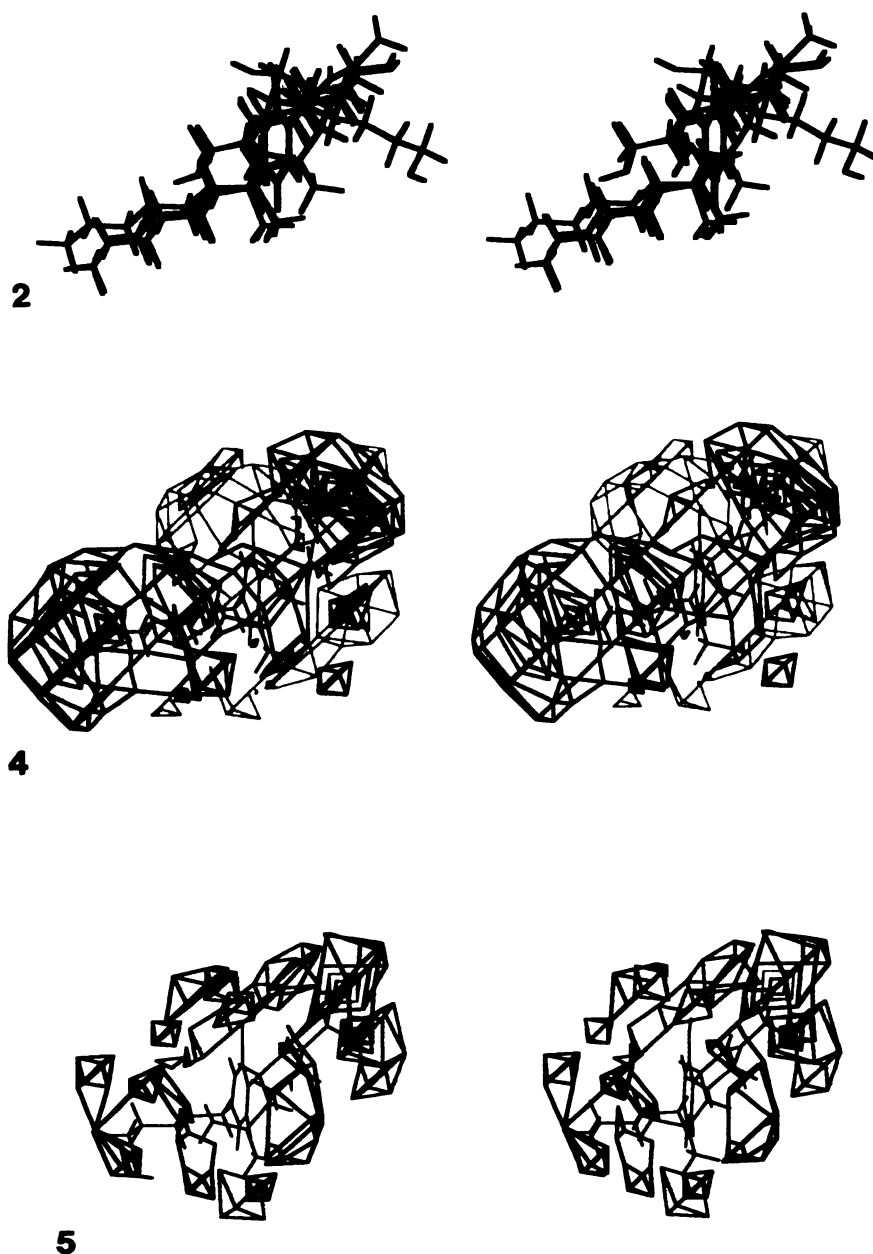
2

4

5

Fig. 2. Stereoview of the alignments of CP-55,244 (*green*), CP-55,940 (*red*), and CP-56,667 (*blue*) with Δ^9-THC (*black*).

Fig. 4. Stereoview of the QSARs for the steric field (van der Waal) CoMFA data, as defined for cannabinoid-induced hypothermia in mice. Plots are colored so that positive coefficients are contoured in *yellow* and *red* and negative coefficients are contoured in *blue* and *green* (in order of increasing magnitude; see Methods). Steric bulk should be moved closer to areas contoured in *green* and *blue* and farther from regions of *red* and *yellow* (assuming that a larger value of the target property is desired). Δ^9-THC is shown in *magenta* within the contour plot.

Fig. 5. Stereoview of the QSARs for the electrostatic field (coulombic) CoMFA data, as defined for cannabinoid-induced hypothermia in mice. Plots are colored so that positive charge should be moved closer to areas contoured in *green* and *blue* and farther from regions of *red* and *yellow* (assuming that a larger value of the target property is desired). Δ^9-THC is shown in *magenta* within the contour plot.

denced by the reasonably high correlation coefficient obtained (0.76). The predicted potencies of the (+)-isomer of the aminoalkylindoles are shown plotted against the actual values. The predicted potencies of the (−)-isomer were >50 μmol/kg, a value higher than the doses tested and shown not to produce a behavioral effect.[2] The limited solubility of WIN-55212-3 prevented the testing of higher doses and precluded the assignment of an actual ED_{50} value in these tests; therefore, the data for this compound were not included in Fig. 7. The predictions for the unsynthesized compound (Fig. 7; predicted cannabinoid

combining structural components of both the WIN series and the DMH series) in decreasing spontaneous activity, tail-flick latency, and rectal temperature and increasing ring-immobility were −1.58, −0.64, −0.21, and −0.25, respectively. These values indicate that this compound should be more potent than Δ^9-THC in producing cannabimimetic effects; however, the synthesis and testing of this compound remain to be performed.

Discussion

The CONCORD program has been reported to be effective for producing three-dimensional structures, due to its simplicity

---

[2] D. R. Compton, unpublished observation.
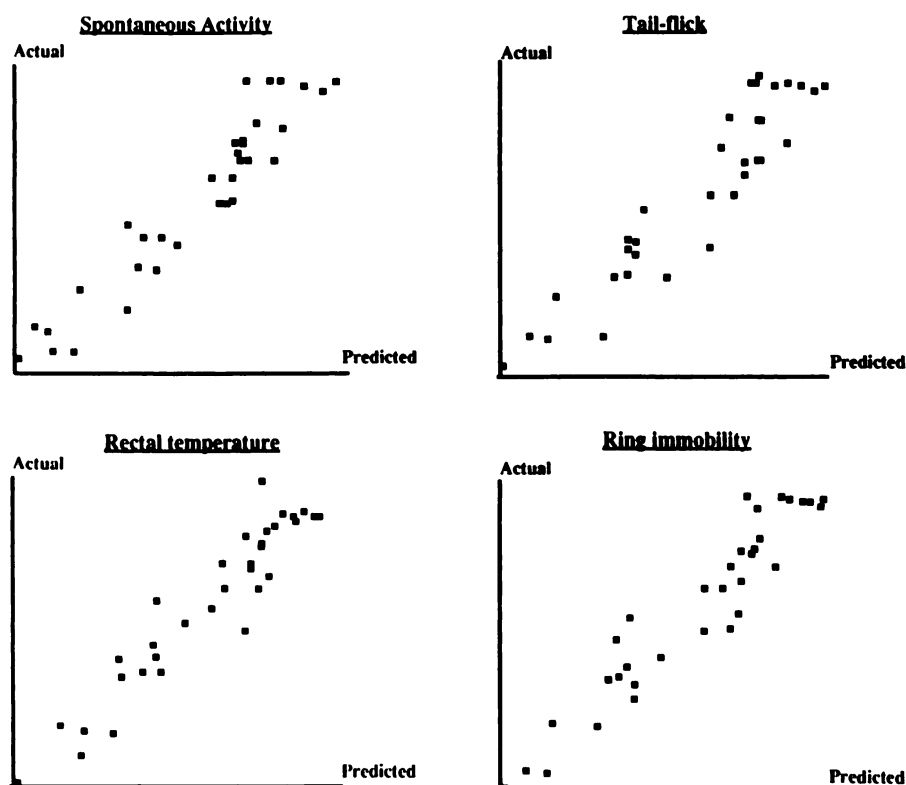
Spontaneous Activity

Tail-flick

Fig. 3. Correlation between the predicted and actual potencies of cannabinoid analogs to produce ring-immobility or catalepsy, inhibit locomotor activity, and produce hypothermia and antinociception (tail-flick latency). Linear regression was a least squares analysis of the predicted potencies of analogs versus their actual potencies [expressed as log (μmol/kg)].

Rectal temperature

Ring immobility

Ring-immobility

$y = -0.75200 + 0.79749x \quad R = 0.86$

Spontaneous Activity

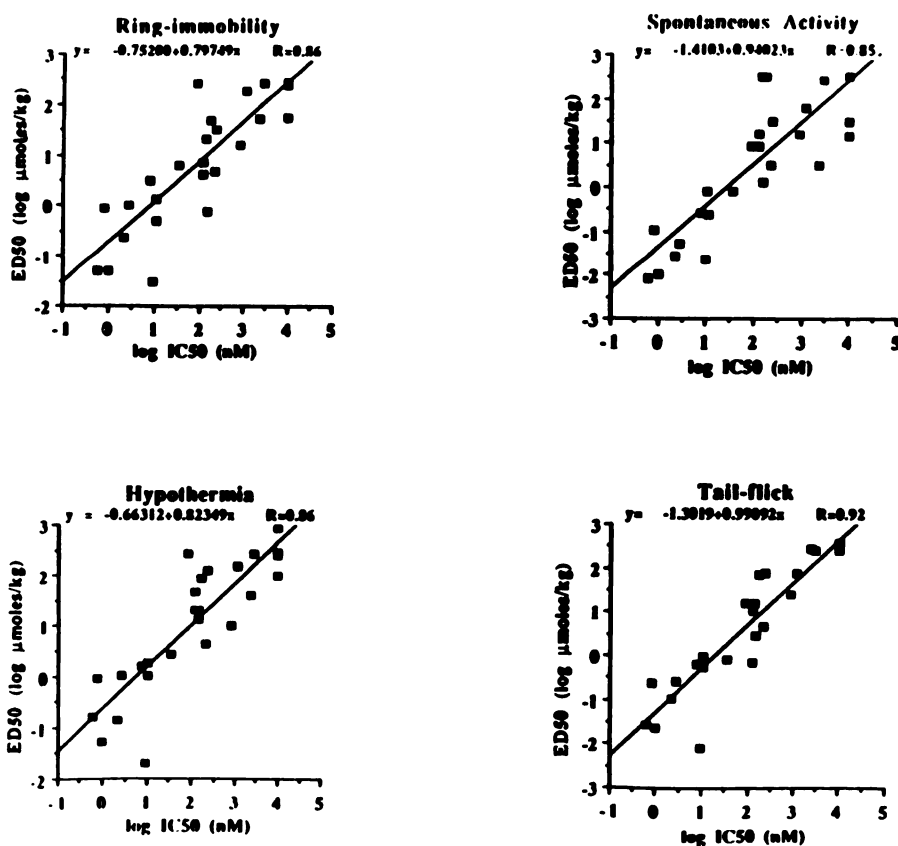$y = -1.4103 + 0.9402x \quad R = 0.85$

Fig. 6. Correlation between the *in vivo* and *in vitro* activities of cannabinoids. The abilities of cannabinoid analogs to decrease spontaneous locomotor activity and rectal temperature and to produce antinociception (tail-flick latency) and ring-immobility (catalepsy) in mice are plotted as log ED_{50} values (μmol/kg) versus the logarithm of their IC_{50} values (nM) in a [^{3}H]CP-55,940 ligand binding assay. Linear regression by least squares analysis.

Hypothermia

$y = -0.66312 + 0.82349x \quad R = 0.86$

Tail-flick

$y = -1.3019 + 0.99092x \quad R = 0.92$

and speed and the quality of the resulting structure (25). The structure of Δ^9-THC generated in this study is in close agreement with the ring structure of Δ^9-tetrahydrocannabinolic acid B (COOH at C4) as determined by X-ray crystallographic analysis (26). The three-dimensional structures of Δ^9-THC and Δ^8-THC generated by Westheimer and extended Hückel mo-

lecular orbital calculations agree with structures determined by proton NMR analysis (27) and by high resolution NMR spectroscopy of Δ^9-THC and Δ^{9-11}-THC (28) and are also consistent with the conformations of these compounds as determined in this study. Furthermore, the conformations of the AC bicyclic and the ACD tricyclic analogs described here are supported by
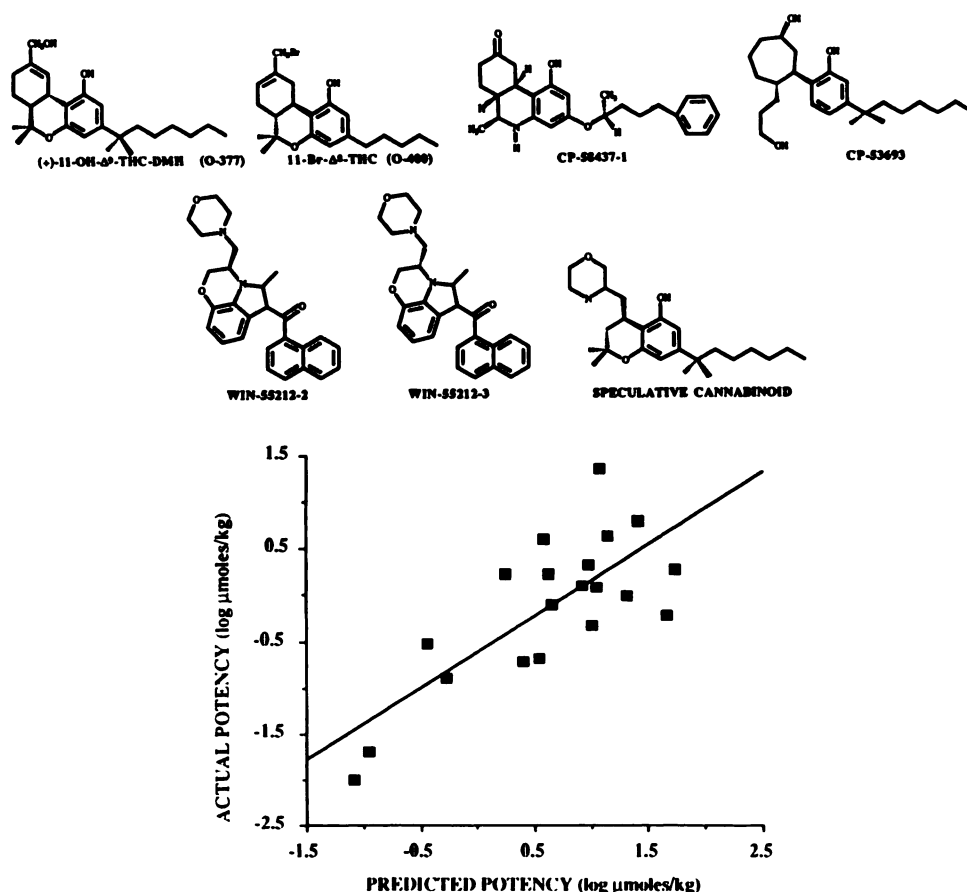
(+)-11-OH-Δ⁹-THC-DMH (O-377)   11-Br-Δ⁸-THC (O-400)   CP-55437-1   CP-53493

WIN-55212-2   WIN-55212-3   SPECULATIVE CANNABINOID

Fig. 7. Correlation between predicted and actual potencies of five cannabinoid compounds not included in the training set. Predicted ED_{50} values of cannabinoid analogs to decrease spontaneous locomotor activity, tail-flick latency, and rectal temperature and to increase ring-immobility in mice are plotted against their actual ED_{50} values, input as μmol/kg. Linear regression by least squares analysis; correlation coefficient determined to be 0.76 ($y = -0.617 + 0.776x$).

MMI calculation of the rotational energy about the bond connecting the aromatic and cyclohexanol rings of CP-47,497, the prototype for the synthesis of the AC and ACD analogs (29). The alignment rules defined in the methods were based upon other structure-activity studies with cannabinoids, which have emphasized the orientation of the phenolic hydroxyl and the presence of a lipophilic side chain as being required for activity (10, 12, 13, 30, 31). The compounds were thus aligned with the aromatic ring and side chain superimposed, which minimized the differences in the molecular fields of the analogs and the template molecule, a procedure that is critical for the generation of relevant molecular field descriptions by CoMFA analysis.

The cross-validated r^2 values obtained here using CoMFA indicate that the model's correlative power with biological potency is intermediate between those of an ideal model ($r^2 = 1.0$) and a model whose accuracy is no different from using the average potency of all compounds in each behavioral assay and using this to predict the activity of unknowns ($r^2 = 0$). It has recently been reported that a cross-validated r^2 of 0.3 indicates the probability of chance correlations of CoMFA data with biological activity will be <5% (32). The r^2 values obtained in this study (all >0.3) indicate a similar (or greater) degree of certainty that the results reported are not based on erroneous correlations. It is this reasonably high cross-validated r^2 that supports the contention that the model obtained in this study will prove useful in predicting the potency of cannabinoid compounds and thereby support the synthesis and testing of cannabinoid analogs. The final analysis of all activities resulted in correlation coefficients that were all approximately 0.9, indicating that, given all the molecules in the table with which

to derive the model, a high degree of predictive power is gained. Additional evidence suggesting that the QSAR analysis reported here will have further potential for characterizing the cannabinoid pharmacophores responsible for the production of cannabimimetic effects is seen in the results obtained with the predictions of compounds not contained in the training set. The correlation between predicted and actual potency of structurally diverse compounds indicates that a robust model has been defined that can continue to incorporate additional compounds into the analysis. This capacity to test and redefine the QSAR with novel compounds provides a means for continually characterizing the ligand-receptor interaction at the molecular level.

The values that were incorporated into the QSAR table included log $P_{o/w}$ values; however, results obtained here using CoMFA analysis indicated that electrostatic factors were weighted the most (approximately 60%), and steric factors accounted for the remainder of the model's correlation between predicted and actual activities. The inability of the log $P_{o/w}$ values to contribute to the predictive power of this model is in agreement with direct linear regression analysis between log $P_{o/w}$ and the log potencies within this series ($r < 0.5$) and with our previous observation that bulk lipophilicity is not directly correlated to the potency of cannabinoid compounds (21). However, the possibility remains that important lipophilic domains exist within the structure of cannabinoids (i.e., the hydrocarbon side chain) that interact with lipophilic sites at, or near, the receptor. Further refinement of the physicochemical parameter measuring lipophilicity is required (e.g., from the lipophilicity of the overall molecule to hydrophobic fragment analysis) in order to detect these possible areas of lipophilic interaction.

The steric properties of cannabinoid analogs that have been determined to be of importance for the production of behavioral effects and for receptor interaction are supported by results reported by others using nonquantitative structure-activity methods. Kriwacki and Makriyannis (28) suggested that differences in potency might be explained by deviations in the planarity of the tricyclic ring systems between analogs. They reported that in Δ^9-THC the C-ring assumes a flattened chair conformation, causing the C9-CH$_3$ to project above the plane of the aromatic ring. Conversely, the C-ring of the less active structural isomer Δ^{9-11}-THC adopts a chair form, as found in cyclohexane, a conformation that projects the C9-CH$_3$ into the plane of the aromatic ring, thereby forming a coplanar conformation with all three rings. Similar findings have been reported in which the conformation of the C9-CH$_3$, as measured by the C11-C9-C1-O torsion angle, has been correlated with activity (33). Steric bulk in or behind the plane of the aromatic ring at the C9-CH$_3$ position, described here to decrease predicted potency, is consistent with these observations. The importance of the C9 substituent, as defined by this model and reported by others in the literature, is reflected by the significant difference between the activities and minimum energy conformations of the two stereoisomers CP-55,940 and CP-56,667. The energy barrier of rotation about the ring junctions is highest when the rings become coplanar. This energy barrier is almost of sufficient magnitude to prevent complete rotation through this barrier and, therefore, the energy of the conformation where CP-56,667 is forced to fit closely with CP-55,940 (and the template molecule) at the C9 position is energetically unfavorable. The importance of the free phenolic hydroxyl group of cannabinoid analogs is also indicated in the steric contour maps and has been previously discussed as being essential for complete activity (10, 12, 13, 30). An additional area where steric forces are predicted to decrease activity is at the position that lies in front of the plane of the aromatic ring at the position of the ring dimethyl groups of Δ^9-THC. This area is one that is occupied by the methyl group on the ring system of the inactive stereoisomers of levonantradol and *N*-methyl-levonantradol, the *n*-propyl alcohol group of (+)-AC, and the D-ring system of (+)-ACD.

The increased potency of compounds having side chains longer than five carbons, such as the dimethylheptyl-containing analogs, was also defined by CoMFA and PLS analysis. The steric contour map shows a large green-contoured area at the end of the side chain, predicting increased potency for those analogs that have extended side chains. This finding is supported by previous work, where the length of the side chain (in a series of bicyclic analogs) has been determined to be optimal for 1,1-dimethylheptyl and 1,1-dimethyloctyl side chains (13). It should be stressed, however, that in the present study the position of the side chain was arbitrarily oriented. Therefore, the results obtained should not be interpreted as indicating the absolute position required for activity, but only the relative dependence of activity on the length of the side chain. The conformation that the side chain obtains during interaction with its active site will remain uncertain until further investigation, including expansion of structure-activity studies to include rigid analogs that effectively orient the side chain of the molecule in various fixed positions. CoMFA analysis of structural variables (such as the added steric bulk required to cause structural rigidity in rotationally restricted analogs) could be

continued in an attempt to maximize the likelihood of producing the correct interpretation given to rigid conformations.

The electrostatic fields of the cannabinoid analogs were seen to be weighted to a slightly greater degree than the steric fields, with regard to the model's ability to fit the potency of the compounds in the analysis. The regions in the electrostatic contour plot that are correlated with predicted potency are predominantly seen around the C11 position of Δ^9-THC. It appears that the electrostatic forces exerted by compounds containing a hydroxyl position corresponding to the C9 or C11 position of Δ^9-THC favor activity, whereas the electrostatic forces exerted by carboxylic acid-containing compounds result in decreased predicted potency. The contour plots suggest that the protons of hydroxyl groups at positions corresponding to the C11 position of Δ^9-THC may interact with an electronegative acceptor atom (e.g., a carboxylic acid functional group) on the receptor. Further expansion and subsequent PLS analysis, an integral part of QSAR analysis, may allow the electrostatic fields to be further characterized and the electrostatic field-activity relationship more readily interpreted.

Because displaying the contoured QSAR coefficients allows visualization of areas where changes in potency are most strongly related to changes in electrostatic and steric fields, these diagrams should be interpretable in terms of receptor structure. The similarity between the contoured steric and electrostatic fields for each dependent variable, and the apparent relationship between the log IC$_{50}$ values and behavioral potency (Fig. 6), suggest that a similar mode of receptor interaction is responsible for the production of the four behavioral effects modeled in this analysis. In fact, the cannabinoid compounds in this analysis typically produced all the effects modeled in this analysis in a similar potency ranking, with relatively few exceptions. In this study, only one compound was seen to possess a dramatically different potency in one behavioral assay when compared with the others. This compound, the 11-fluoro-derivative of Δ^8-THC, requires further study in order to determine why it produces antinociceptive effects at doses that fail to produce the other three effects. Because the autoradiographic analysis of [^{3}H]CP-55,940 shows a wide distribution of cannabinoid binding sites throughout the CNS (6), interaction with this putative cannabinoid receptor (or a similar mode of interaction with receptor subtypes) in different regions of the CNS may be responsible for the production of these varied behavioral effects. However, if the biological activities are produced through interaction with more than one neuronal substrate, the results of this study indicate that the structural and electrostatic properties required for producing these effects are similar (within this series of compounds).

The utility of the CoMFA technique for the QSAR analysis of other classes of compounds is mostly unknown, even though a number of individuals have been reported as experiencing a high degree of satisfaction with CoMFA analysis of their own data (32). In general, it can be stated that with PLS analysis chance correlation occurs if a large proportion of the columns will simultaneously correlate with the dependent variable, a low probability that decreases as the number of columns increases. Thus, substituting PLS for regression reduces the probability of accepting a chance correlation while increasing the probability that a "true" correlation involving only a few independent variables will go undetected. The effect of CoMFA variables such as the number of compounds, the number of cross-validation groups, the number of compounds aligned "in-

correctly," the effect of the size and charge of the probe atom, and the grid-spacing and positioning on the cross-validated r^2 obtained by PLS has been previously evaluated (14, 32). Molecular alignment is the most important factor determining the success of a CoMFA QSAR analysis, but it is also a parameter that is easily influenced by investigator bias when performed manually. The development of an automated alignment procedure based on the minimization of the RMS difference (field-fitting) in molecular fields has been recently implemented in SYBYL molecular modeling software and may eliminate the need for the identification of point-to-point correspondences in molecules to be aligned. Unfortunately, the utility of this procedure remains to be determined in a comprehensive manner. Finally, it should be stated that the model derived by CoMFA may not be describing the complete pharmacophore (i.e., the entire active site of the receptor) but, rather, a subsection of the pharmacophore. Also, the model obtained will not account for the effect of structural and bulk waters on the binding of compounds to the receptor. Given the constraints imposed by the training set, the model may incorrectly predict the activity of a compound that is dramatically different from this set. Alternatively, there also may be noncannabinoid compounds that would fit in the pharmacophore model and erroneously be predicted to possess cannabinoid-like pharmacological activity. These limitations serve to underscore the importance of predicting unknowns, testing the unknown compounds, and incorporating these compounds into the model by repeating the QSAR analysis.

Acknowledgments

References

1. Makriyannis, A., A. Banijamali, C. Van der Schyf, and H. Jarrell. Interactions of cannabinoids with membranes: the role of cannabinoid stereochemistry and absolute configuration and the orientation of Δ^9-THC in the membrane bilayer. *Natl. Inst. Drug Abuse Res. Monogr. Ser.* **79**:123–133 (1987).
2. Hillard, C. J., R. A. Harris, and A. S. Bloom. Effects of the cannabinoids on physical properties of brain membranes and phospholipid vesicles: fluorescence studies. *J. Pharmacol. Exp. Ther.* **232**:579–588 (1985).
3. Gill, E. W., and D. K. Lawrence. The physicochemical mode of action of tetrahydrocannabinol on cell membranes, in *The Pharmacology of Marihuana* (M. C. Braude and S. Szara, eds.). Raven Press, New York, 147–155 (1976).
4. Martin, B. R. Cellular effects of cannabinoids. *Pharmacol. Rev.* **38**:45–74 (1986).
5. Harris, L. S., R. A. Carchman, and B. R. Martin. Evidence for the existence of specific cannabinoid binding sites. *Life Sci.* **22**:1131–1138 (1978).
6. Herkenham, M., A. B. Lynn, M. D. Little, M. R. Johnson, L. S. Melvin, B. R. DeCosta, and K. C. Rice. Cannabinoid receptor localization in the brain. *Proc. Natl. Acad. Sci. USA* **87**:1932–1936 (1990).
7. Devane, W. A., F. A. Dysarz, M. R. Johnson, L. S. Melvin, and A. C. Howlett. Determination and characterization of a cannabinoid receptor in rat brain. *Mol. Pharmacol.* **34**:605–613 (1988).
8. Matsuda, L. A., S. J. Lolait, M. J. Brownstein, A. C. Young, and T. L. Bonner. Structure of a cannabinoid receptor and functional expression of the cloned cDNA. *Nature (Lond.)* **346**:561–564 (1990).
9. Edery, H., Y. Grunfeld, Z. Ben-Zvi, and R. Mechoulam. Structural requirements for cannabinoid activity. *Ann. N. Y. Acad. Sci.* **191**:40–53 (1971).
10. Razdan, R. K. Structure-activity relationships in cannabinoids. *Pharmacol. Rev.* **38**:75–150 (1986).
11. Binder, M., and I. Franke. Is there a cannabinoid receptor? Current perspectives and approaches to the elucidation of the molecular mechanism of action of the psychotropic constituents of *Cannabis sativa L.*, in *Neuroreceptors* (F. Hucho, ed.). Walter de Gruyter, Berlin, 151–161 (1982).
12. Howlett, A. C., M. R. Johnson, L. S. Melvin, and G. M. Milne. Nonclassical cannabinoid analgetics inhibit adenylate cyclase: development of a cannabinoid receptor model. *Mol. Pharmacol.* **33**:297–302 (1988).
13. Johnson, M. R., and L. S. Melvin. The discovery of nonclassical cannabinoid analgetics, in *Cannabinoids as Therapeutic Agents* (R. Mechoulam, ed.). CRC Press, Boca Raton, FL, 121–145 (1986).
14. Cramer, R. D., D. E. Patterson, and J. D. Bunce. Comparative molecular field analysis (CoMFA). 1. Effect of shape on binding of steroids to carrier proteins. *J. Am. Chem. Soc.* **110**:5959–5967 (1988).
15. Cramer, R. D., J. D. Bunce, D. E. Patterson, and I. E. Frank. Crossvalidation, bootstrapping, and partial least squares compared with multiple regression in conventional QSAR studies. *Quant. Struct.-Act. Relat.* **7**:18–25 (1988).
16. Cramer, R. D., D. E. Patterson, and J. D. Bunce. Recent advances in comparative molecular field analysis (CoMFA), in *QSAR: Quantitative Structure-Activity Relationships in Drug Design* (J.-L. Fauchere, ed.), Alan R. Liss, Inc., New York, 161–165 (1989).
17. Mayer, D., C. B. Naylor, I. Motoc, and G. R. Marshall. A unique geometry of the active site of angiotensin-converting enzyme consistent with structure-activity studies. *J. Comput. Aided Mol. Des.* **1**:3–16 (1987).
18. Leuschner, J. T. A., D. R. Wing, D. J. Harvey, G. A. Brent, C. E. Dempsey, A. Watts, and W. D. M. Paton. The partitioning of Δ^1-tetrahydrocannabinol into erythrocyte membranes *in vivo* and its effect on membrane fluidity. *Experientia (Basel)* **40**:866–868 (1984).
19. Lawrence, D. K., and E. W. Gill. The effects of Δ^1-tetrahydrocannabinol and other cannabinoids on spin-labeled liposomes and their relationship to mechanisms of general anesthesia. *Mol. Pharmacol.* **11**:595–602 (1975).
20. Roth, S. H., and P. J. Williams. The non-specific membrane binding properties of Δ^9-tetrahydrocannabinol and the effects of various solubilizers. *J. Pharm. Pharmacol.* **31**:224–230 (1979).
21. Thomas, B. F., D. R. Compton, and B. R. Martin. Characterization of the lipophilicity of natural and synthetic analogs of Δ^9-tetrahydrocannabinol and its relationship to pharmacological potency. *J. Pharmacol. Exp. Ther.* **255**:624–630 (1990).
22. Ghose, A. K., and G. M. Crippen. Modeling the benzodiazepine receptor binding site by the general three-dimensional structure-directed quantitative structure-activity relationship method REMOTEDISC. *Mol. Pharmacol.* **37**:725–734 (1990).
23. Little, P. J., D. R. Compton, M. R. Johnson, L. S. Melvin, and B. R. Martin. Pharmacology and stereoselectivity of structurally novel cannabinoids in mice. *J. Pharmacol. Exp. Ther.* **247**:1046–1051 (1988).
24. Compton, D. R., M. R. Johnson, L. S. Melvin, and B. R. Martin. Pharmacological profile of a series of bicyclic cannabinoid analogs: classification as cannabimimetic agents. *J. Pharmacol. Exp. Ther.*, in press.
25. Cohen, N. C., J. M. Blaney, C. Humblet, P. Gund, and D. C. Barry. Molecular modeling software and methods for medicinal chemistry. *J. Med. Chem.* **33**:883–894 (1990).
26. Tolenaere, J. P., H. Moereels, and L. A. Raymaekers. *Atlas of the Three-Dimensional Structure of Drugs*. Elsevier, New York, 232 (1979).
27. Archer, R. A., D. B. Boyd, P. V. Demarco, I. J. Tyminski, and N. L. Allinger. Structural studies of cannabinoids: a theoretical and proton magnetic resonance analysis. *J. Am. Chem. Soc.* **92**:5200–5206 (1970).
28. Kriwacki, R. W., and A. Makriyannis. The conformational analysis of Δ^9- and $\Delta^{9,11}$-tetrahydrocannabinols in solution using high resolution nuclear magnetic resonance spectroscopy. *Mol. Pharmacol.* **35**:495–503 (1989).
29. Melvin, L. S., M. R. Johnson, C. A. Harbert, G. M. Milne, and A. Weissman. A cannabinoid derived prototypical analgesic. *J. Med. Chem.* **27**:67–71 (1984).
30. Semus, S. F., and B. R. Martin. A computer graphic investigation into the pharmacological role of the THC-cannabinoid phenolic moiety. *Life Sci.* **46**:1781–1785 (1990).
31. Binder, M., F.-J. Witteler, B. Schmidt, I. Franke, E. Bohnenberger, and H. Sanderman. Triglyceride/phospholipid partitioning and pharmacokinetics of some natural and semi-synthetic cannabinoids: further evidence for the involvement of specific receptors in the mediation of the psychotropic effects of *delta*-1-THC and *delta*-6-THC, in *The Cannabinoids: Chemical, Pharmacologic, and Therapeutic Aspects* (S. Agurell, W. L. Dewey, and R. E. Willette, eds.). Academic Press, Inc., New York, 709–727 (1984).
32. Clark, M., R. D. Cramer III, D. M. Jones, D. E. Patterson, and P. E. Simeroth. Comparative molecular field analysis (CoMFA). 2. Toward its use with 3D-structural databases. *Tetrahed. Computer. Methods* **3**:47–59 (1990).
33. Reggio, P. H., K. V. Greer, and S. M. Cox. The importance of the orientation of the C9 substituent to cannabinoid activity. *J. Med. Chem.* **32**:1630–1635 (1989).